Acta Mechanica Solida Sinica, Vol. 21, No. 2, April, 2008 ISSN 0894-9166
Published by AMSS Press, Wuhan, China. DOI: 10.1007/s10338-008-0820-7

NONLINEAR RESPONSES OF A FLUID-CONVEYING PIPE EMBEDDED IN NONLINEAR ELASTIC FOUNDATIONS**

Qin Qian Lin Wang* Qiao Ni

(*Department of Mechanics, Huazhong University of Science and Technology, Wuhan* 430074*, China*)

Received 6 September 2007; revision received 26 February 2008

ABSTRACT The nonlinear responses of planar motions of a fluid-conveying pipe embedded in nonlinear elastic foundations are investigated via the differential quadrature method discretization (DQMD) of the governing partial differential equation. For the analytical model, the effect of the nonlinear elastic foundation is modeled by a nonlinear restraining force. By using an iterative algorithm, a set of ordinary differential dynamical equations derived from the equation of motion of the system are solved numerically and then the bifurcations are analyzed. The numerical results, in which the existence of chaos is demonstrated, are presented in the form of phase portraits of the oscillations. The intermittency transition to chaos has been found to arise.

KEY WORDS fluid-conveying pipe; nonlinear elastic foundation; chaotic motion; bifurcation; differential quadrature method discretization (DQMD)

I. INTRODUCTION

A theory for the dynamics of fluid-conveying pipes, both straight and curved, is of considerable interest in many fields. Its applications include the design of ocean pipelines, pump discharge lines, propellant lines and reactor system components etc. As discussed in a review[1], where extensive references may be found, the fluid-conveying pipe has become a paradigm in the study of stability and nonlinear systems. Variants of pipe systems have been shown to exhibit complex dynamics and chaotic motions, as described below.

Up to now, straight pipes conveying fluid have been investigated extensively. Tang and Dowell[2] considered a straight pipe with an inset steel strip and two equal-spaced permanent magnets on either side, by exerting strong nonlinear forces on the pipe and buckling it into one of the two potential wells on either side of the pipe. If the fluid velocity is sufficiently high over the critical value for flutter about the buckled state, the system would develop chaotic oscillations. This may be the first study in which chaos was detected in fluid-conveying pipe systems. Almost at the same time, Paidoussis et al.[3–6] undertook a combined theoretical and experimental study of an autonomous system of a cantilevered straight fluid-conveying pipe interacting with motion constraints somewhere along the length of the pipe. The same system was studied by Ni & Huang[7] via increment harmonic balance method (IHBM), showing some interesting nonlinear characteristic of the pipe system.

* Corresponding author. E-mail: wanglinfliping@sohu.com

** Project supported by the National Natural Science Foundation of China (No.10772071) and the Scientific Research Foundation of HUST (No.2006Q003B).

In 1997, a similar dynamical system was studied by Jin[8]. In Jin's model, the pipe is also restrained by motion constraints but with a linear spring support attached to the pipe at the restrained point (shown in Fig.1(a)). It should be noted that, Jin's model becomes the same one as studied by Paidoussis et al.[3–6] when the linear spring support is removed. The analytical model, after Galerkin discretization to two d.o.f., showed some unexpected results. It was found that, the linear spring support has a significant effect on the nonlinear dynamics and a codimension two bifurcation might occur. The same system was recently re-examined by Wang & Ni[9], utilizing the differential quadrature method discretization (DQMD) to discretize the pipe model. Similar results as foregoing were obtained, showing good agreement with those obtained by Jin[8]. Very recently, Wang & Ni[10] investigated the nonlinear dynamics of a vertical standing straight fluid-conveying pipe with motion constraints and a linear spring support, in which chaos was found as well as some other results.

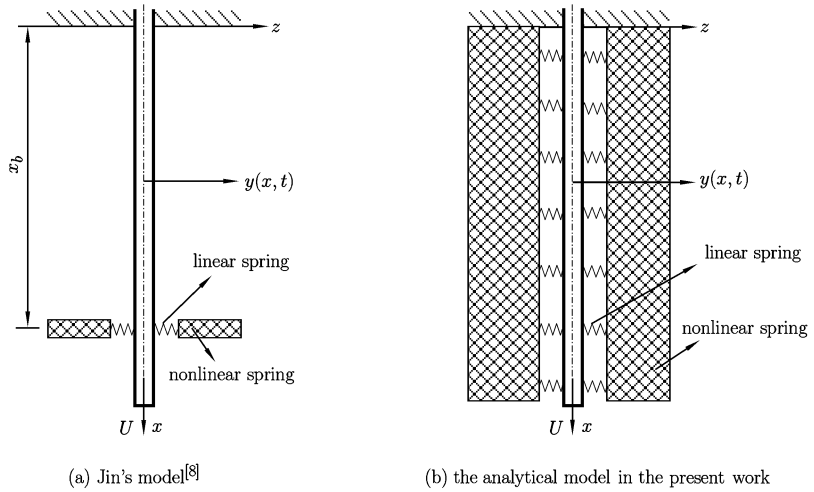

(a) Jin's model[8] (b) the analytical model in the present work

Fig. 1. Schematic of fluid-conveying pipes.

For curved fluid-conveying pipes, it was shown that they can exhibit interesting dynamic responses including chaotic behaviors. Ni et al.[11] studied a curved pipe conveying fluid embedded in distributed nonlinear foundations, in which chaotic transients were examined via numerical simulations. Afterwards, the dynamics of a semi-circular fluid-conveying pipe subjected to motion constraints, modeled as cubic springs, was recently studied[12]. Based on the extensive calculations as mentioned above, this curved pipe system was found to exhibit regions of chaotic motions.

Therefore, it is clear that the basic system of a pipe conveying fluid[13] and variants thereof are capable of displaying extremely rich and variegated dynamical behaviors. In the foregoing references cited, the straight fluid-conveying pipes were restrained by motion constraints somewhere along the length of the pipe, with or without the linear spring support. In practice, however, such pipes are always embedded in a distributed nonlinear elastic medium. Therefore, a model of the distributed nonlinear elastic medium must be included in the governing differential equation. The present paper concerns the nonlinear dynamics of a straight pipe conveying fluid that is embedded in distributed nonlinear elastic foundations. In the analytical model, the fluid-conveying pipe is initially straight. The equation of motion of the pipe is firstly recasted into a set of ordinary differential equations by DQMD. The simulated system is then studied, with special attention to the possible bifurcations and chaotic motions. Numerical results show that the route to chaos is via an intermittency transition.

II. THE GOVERNING PARTIAL DIFFERENTIAL EQUATION

Figure 1(b) shows the schematic of the fluid-conveying pipe considered in this paper. The undisturbed flow of incompressible fluid through the inner pipe follows the direction of the axis x, entering at $x = 0$. Transverse deflections occur in the vertical plane taking the direction of the axis z. The pipe has a specific mass m and a bending stiffness EI. The fluid flowing through the pipe has a specific mass

M. Moreover, the pipe is conveying the fluid with a mean velocity U. For such a fluid-pipe interaction system, the effect of the nonlinear elastic foundation can be written as the restraining force:

$$F = K_1 y + K_2 y^3 \tag{1}$$

where K_1 is the stiffness of the elastic spring, K_2 is the stiffness of the cubic spring.

In this study, the geometrical nonlinearity will not be considered since the deflection of the pipe is sufficiently small. The only nonlinearity in the equation of motion is associated with the nonlinear elastic foundations. Then, the equation of motion for the fluid-conveying pipe may be written as

$$\begin{aligned} aEI\frac{\partial^5 y}{\partial x^4 \partial t} + EI\frac{\partial^4 y}{\partial x^4} + [MU^2 - (M+m)(L-x)g]\frac{\partial^2 y}{\partial x^2} + (M+m)g\frac{\partial y}{\partial x} \\ +2MU\frac{\partial^2 y}{\partial x \partial t} + C\frac{\partial y}{\partial t} + (M+m)\frac{\partial^2 y}{\partial t^2} + K_1 y + K_2 y^3 = 0 \end{aligned} \tag{2}$$

where C is the external damping coefficient, L is the length of the pipe, g represents the acceleration due to gravity, a is the coefficient of Kelvin-Voigt viscoelastic damping, $y(x,t)$ is the lateral deflection of the pipe, assumed to be very small with respect to L, x is the axis defined in Fig.1, and t is time. Since the only non-linearity in Eq.(2) is associated with the nonlinear elastic foundations, Eq.(2) should be valid provided that pipe motions are not too large.

Here, it ought to recall that, in the notable work by Jin[8], a similar fluid-conveying pipe system was analyzed. In Jin's model, the straight pipe was restrained by a single nonlinear elastic support placed somewhere along the pipe axis as shown in Fig.1(a). However, the analytical model in the present paper is associated with a fluid-conveying pipe restrained by distributed nonlinear supports. The equation for a fluid-conveying pipe restrained by a single nonlinear elastic support has been obtained in Ref.[8] and can be written as

$$\begin{aligned} aEI\frac{\partial^5 y}{\partial x^4 \partial t} + EI\frac{\partial^4 y}{\partial x^4} + [MU^2 - (M+m)(L-x)g]\frac{\partial^2 y}{\partial x^2} + (M+m)g\frac{\partial y}{\partial x} \\ +2MU\frac{\partial^2 y}{\partial x \partial t} + C\frac{\partial y}{\partial t} + (M+m)\frac{\partial^2 y}{\partial t^2} + \left(K_1 y + K_2 y^3\right)\delta(x - x_b) = 0 \end{aligned} \tag{3}$$

where $\delta(x - x_b)$ is the Dirac delta function, and x_b is the location coordinate of the single nonlinear elastic support.

Nondimensional quantities used in this work are defined as follows:

$$\begin{aligned} &\tau = \frac{\sqrt{EI/(M+m)}t}{L^2}, \quad u = \sqrt{\frac{M}{EI}}UL, \qquad \eta = \frac{y}{L}, \qquad \xi = \frac{x}{L} \\ &\beta = \frac{M}{M+m}, \qquad \gamma = \frac{(M+m)gL^3}{EI}, \qquad k_1 = \frac{KL^3}{EI}, \quad k_2 = \frac{KL^5}{EI} \\ &\alpha = \frac{\sqrt{EI/(M+m)}a}{L^2}, \quad c = \frac{CL^2}{\sqrt{EI/(M+m)}} \end{aligned}$$

Then, Eq.(2) can be written in the dimensionless form

$$\alpha\frac{\partial^5 \eta}{\partial \xi^4 \partial \tau} + \frac{\partial^4 \eta}{\partial \xi^4} + [u^2 - \gamma(1-\xi)]\frac{\partial^2 \eta}{\partial \xi^2} + \gamma\frac{\partial \eta}{\partial \xi} + 2\sqrt{\beta}u\frac{\partial^2 \eta}{\partial \xi \partial \tau} + \frac{\partial^2 \eta}{\partial \tau^2} + c\frac{\partial \eta}{\partial \tau} + k_1\eta + k_2\eta^3 = 0 \tag{4}$$

This equation holds for a sufficiently long and slender pipe for small pipe deflections, where the Euler-Bernoulli beam theory is applicable.

The boundary conditions to be satisfied are as follows:

$$\text{at} \quad \xi = 0: \qquad \eta = \frac{\partial \eta}{\partial \xi} = 0 \tag{5}$$

$$\text{at} \quad \xi = 1: \qquad \frac{\partial^2 \eta}{\partial \xi^2} = \frac{\partial^3 \eta}{\partial \xi^3} = 0 \tag{6}$$

III. TRANSFORMATION OF PDE INTO A SET OF ODES

For a straight pipe conveying fluid, the conventional method to discretize the infinite dimensional model is the Galerkin's technique, with suitable beam eigenfunctions and the corresponding generalized coordinates. However, complex integral operations are needed if using the Galerkin expansion and modal truncation techniques. To simplify the process, a novel DQMD method is used here to transform the Partial differential equation (PDE) into a set of ordinary differential equations (ODEs). This method has been effectively used to analyze many dynamical systems[9–11, 14].

The DQMD is a numerical method to discretize structures in one or two space variables. This method approximates the partial derivative of a function with respect to a space variable at given discrete points as a weighted linear sum of the function values at all discrete points. Then, a differential quadrature approximation at the i-th discrete point on a grid is given by

$$L_k\{f(x)\}_i = \sum_{j=1}^{N} A_{ij}^{(k)} f(x_j) \qquad (i = 1, 2, \cdots, N) \tag{7}$$

Here $L\{\}$ is a linear operator applied to a function $f(x)$, x is the independent variable and x_j are the sample points obtained by dividing the x-variable into N discrete values; $f(x_j)$ are the function values at these points, A_{ij} are the weights attached to these function values. It ought to be noted that the weighting coefficients A_{ij} have been explicitly obtained and used in papers[9–11, 14] and will be directly applied in the current work.

For the pipe system considered here, the discrete points are in the domain of ξ. By using the following way to discretize $\xi(0 \le \xi \le 1)$, one obtains the unequally spaced sampling points with two adjacent δ-points ($\delta = 10^{-6} \sim 10^{-3}$) at the two boundary ends, namely

$$\begin{aligned} &\xi_1 = 0, \qquad \xi_2 = \delta, \quad \xi_{N-1} = 1 - \delta \\ &\xi_N = 1, \qquad \xi_i = \frac{1}{2}\left[1 - \cos\left(\frac{i-3}{N-4}\pi\right)\right] \qquad (i = 3, 4, \cdots, N-2) \end{aligned} \tag{8}$$

Hence, applying the DQMD to Eqs.(4)-(6) yield

$$\begin{aligned} \sum_{j=1}^{N}\{A_{ij}^{(4)} + [u^2 - \gamma(1-\xi_i)]A_{ij}^{(2)} + \gamma A_{ij}^{(1)}\}\eta_j + \sum_{j=1}^{N}(\alpha A_{ij}^{(4)} + 2\sqrt{\beta}u A_{ij}^{(1)})\dot{\eta}_j \\ + c\dot{\eta}_i + k_1\eta_i + k_2\eta_i^3 + \ddot{\eta}_i = 0 \qquad (i = 3, 4, \cdots N-2) \end{aligned} \tag{9}$$

and

$$\eta_1 = 0, \qquad \sum_{j=1}^{N} A_{2j}^{(1)}\eta_j = 0, \qquad \sum_{j=1}^{N} A_{N-1j}^{(2)}\eta_j = 0, \qquad \sum_{j=1}^{N} A_{Nj}^{(3)}\eta_j = 0 \tag{10}$$

By collecting Eqs.(9) and (10), the dynamical equations of motion can be written in the following form:

$$\boldsymbol{M}\ddot{\boldsymbol{\eta}} + \boldsymbol{G}\dot{\boldsymbol{\eta}} + \boldsymbol{K}\boldsymbol{\eta} = \boldsymbol{Q} \tag{11}$$

where $\boldsymbol{\eta}$ is the dynamic displacement vector, $\boldsymbol{M}$, $\boldsymbol{G}$ and $\boldsymbol{K}$ are the generalized mass matrix, damping matrix and stiffness matrix, respectively. The matrix elements of $\boldsymbol{G}$ and $\boldsymbol{K}$ are the functions of system parameters, i.e. the dimensionless flow velocity v and mass ratio β. $\boldsymbol{Q}$ is the external applied load vector, and the elements of $\boldsymbol{Q}$ are all equal to zero for the present system.

Equation (11) is the non-linear dynamic equation of motion for the fluid-conveying pipe. By solving this equation one can study the dynamical behavior of the system and determinate whether the chaotic motions occur or not under the specified conditions.

IV. NUMERICAL ANALYSIS

In the following discussion, the dynamic behavior with the variant of system parameters is investigated with great interest. Some numerical analysis was done to explore the more details. Based on the DQMD, solutions of Eq.(11) were obtained by using the Newmark method and the Newton-Raphson iteration, with a time step size of 0.0025; the initial conditions employed were $\eta(i,0) = -10^{-6}$, $\ddot{\eta}(i,0) = 10^{-5}$ $(i = 3, 4, \cdots, N)$. In the following calculations, the sampling point number for DQMD is chosen to be $N = 9$.

4.1. Bifurcation Diagram

Numerical simulations produced the bifurcation diagram of Fig.2 for a set of system parameters defined as: $\gamma = 10$, $k_1 = 100$, $k_2 = 1000000$, $\alpha = 0.005$, $c = 0.2$ and $\beta = 0.2$. In this figure, the displacement plotted in the ordinate is the amplitude of the free-end displacement of the pipe; the variable parameter is the dimensionless flow velocity u. Moreover, in the calculations, the transient solutions were discarded. Whenever the free-end velocity was zero, the displacement at the free end was recorded — thus produce both negative and positive values, as shown in Fig.2.

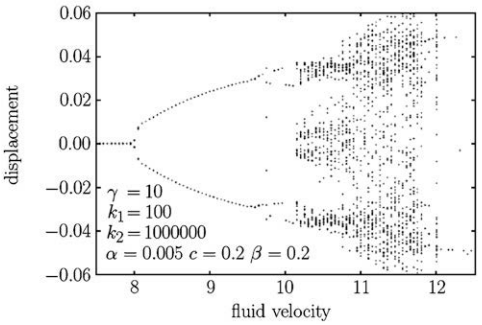

Fig. 2 Bifurcation diagram: the tip (end) displacement as a function of fluid velocity u.

In Fig.2, it can be denoted $u_H \cong 7.83$ as the Hopf bifurcation point. When $u < u_H$, the fluid-conveying pipe is at a stable fixed point. Thus the displacements and velocities of the free-end of the pipe are zero. However, after the Hopf bifurcation point, symmetric limit cycle motion occurs when $u \geq u_H$. Moreover, the radius of the limit cycle is increased with increasing fluid velocity. It is of interest that this symmetric limit cycle motion is replaced by an asymmetric one at $u = u_P \cong 9.58$, which corresponds to the pitchfork bifurcation. As shown in Fig.2, there is a small region of period-3 motion embedded within the asymmetric limit cycle motion region. At $u \approx 10.128$, chaotic motion occurs. However, the route to chaos can not be clearly recognized from the bifurcation diagram. Finally, with the gradual increasing when u is reasonably high (e.g. $u = 12.05$), a stable focus occurs with negative or positive displacement. In this case the pipe end may settle down onto one side of the foundations.

4.2. Hopf Bifurcation Point

As mentioned in the previous section, Hopf bifurcation may occur at $u = u_H$. However, all the system parameters are fixed as mentioned in §4.1 and only the dimensionless flow velocity u is gradually increased.

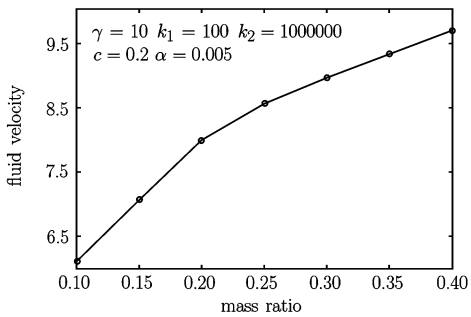

Fig. 3. Critical fluid velocity corresponding to Hopf bifurcation *vs.* mass ratio β.

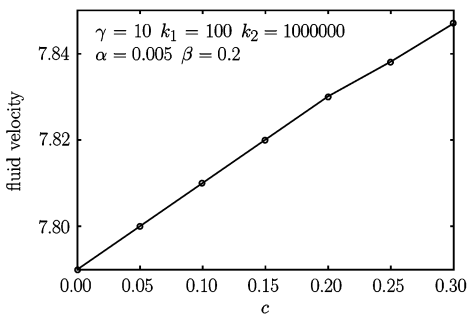

Fig. 4. Critical fluid velocity corresponding to Hopf bifurcation *vs.* c.

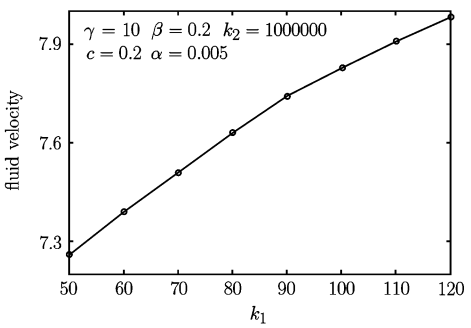

Fig. 5. Fluid velocity corresponding to Hopf bifurcation *vs.* k_1.

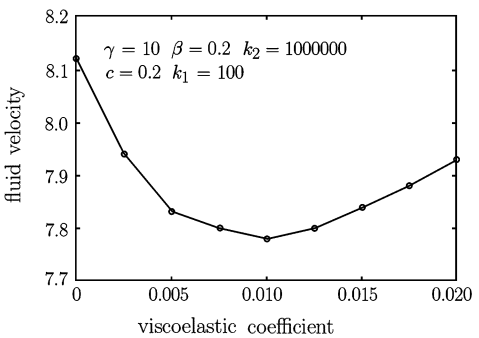

Fig. 6. Fluid velocity corresponding to Hopf bifurcation *vs.* α.

The main concern here is the effects of several other key parameters (i.e. β, c, k_1 and α) on the critical fluid velocity corresponding to the Hopf bifurcation point. The results are shown in Figs.3-6. It is seen that, the effect of these four parameters on the critical fluid velocity corresponding to Hopf bifurcation is significant. However, it is found that k_2 only affects the amplitude of the resultant motions, implying that the Hopf bifurcation point and the global dynamics of the system are insensitive to k_2.

4.3. Typical Motions

It is instructive to look at phase-plane portraits associated with various values of u, corresponding to different dynamical behavior as discussed in §4.1. For this purpose, sample results are shown in Fig.7. For $u < u_H$, it can be seen in Fig.7(a) that the origin is a stable fixed point towards which the trajectory gravitates. In Fig.7(b) for $u > u_H$, the trajectory is towards a stable symmetric limit cycle. In Fig.7(h), the motion is clearly a stable focus with negative displacement. The other few images in Fig.7, in which the initial transients have been omitted for clarity, represent different motions with (c) showing a period-1 motion; (d) and (g) showing period-3 motions; (e) and (f) showing chaotic motions.

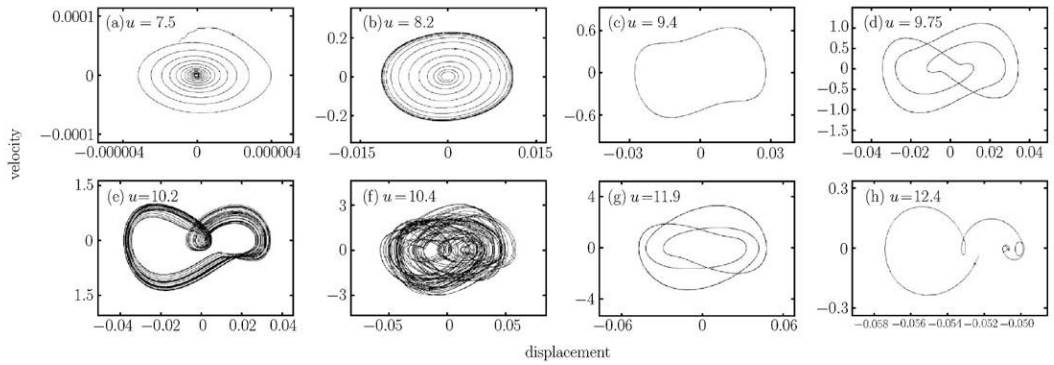

Fig. 7. Phase-plane portraits for $\gamma = 10$, $k_1 = 100$, $k_2 = 1000000$, $\alpha = 0.005$, c=0.2, $\beta = 0.2$, and different values of u.

4.4. Route to Chaos

As discussed above, the onset of chaotic motion occurs at $u \approx 10.128$. It is difficult to determine the route to chaos only from the bifurcation diagram since the calculating interval Δu is relatively big. Based on extensive calculations with small Δu, the intermittency transition to chaos can be found in

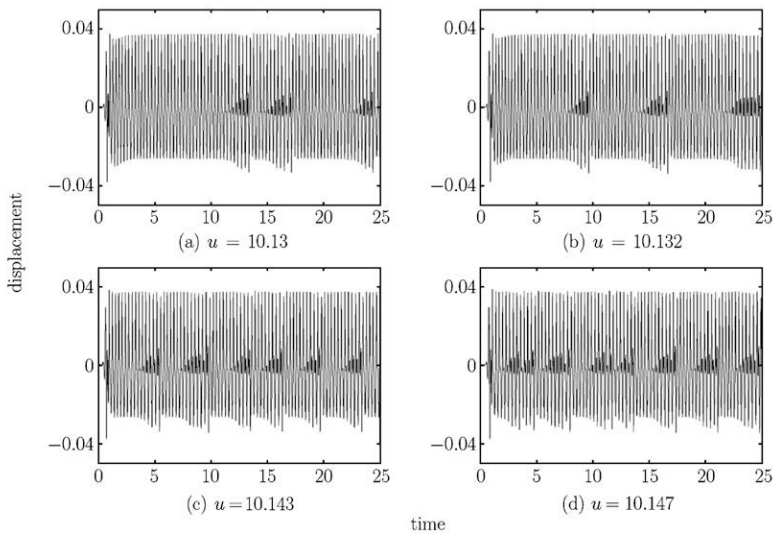

Fig. 8. Time responses for different values of u.

the parameter space of u. The intermittency transition is represented in Fig.8. In Figs.8(a) and (b), the time responses of the vibrations for the system show that period-1 and chaotic motions may occur alternately along the time axis. However, the durations of each period-1 motions can be different from each other, so does for the chaotic motions of the system. With increasing u, the durations of each period-1 motions become shorter, as shown in Figs.8(c) and (d), and the chaotic regime dominates the vibrations of the system.

V. CONCLUSIONS

The main contributions of this paper lie in three aspects. First, an analytical model of the dynamical system was elaborated, considering the nonlinearity induced by the impact between the pipe and the nonlinear elastic foundations and retaining its essential simplicity of the equation of motion. This equation of motion was further reduced using DQMD. The second important contribution of this study is the analysis of bifurcations for the vibrating system. Based on numerical calculations, the bifurcation diagram shows that the system considered may undergo extremely rich and variegated dynamical behaviors such as periodic and chaotic motions. Moreover, the effect of several key system parameters on the Hopf bifurcations is shown to be significant. The third major contribution is the determination of the route to chaos in the parameter region of u. This was done by choosing much smaller calculating interval Δu and the intermittency transition to chaos has been found via extensive calculations.

References

[1] Païdoussis,M.P., Flow-induced instabilities of cylindrical structures. *Applied Mechanics Review*, 1987, 40: 163-175.

[2] Tang,D.M. and Dowel,E.H., Chaotic oscillations of a cantilevered pipe conveying fluid. *Journal of Fluids and Structures*, 1988, 2: 263-283.

[3] Païdoussis,M.P. and Moon,F.C., Non-linear and chaotic fluidelastic vibrations of a flexible pipe conveying fluid. *Journal of Fluids and Structures*, 1988, 3: 567-591.

[4] Païdoussis,M.P., Li,G.X. and Moon,F.C., Chaotic oscillations of the autonomous system of a constrained pipe conveying fluid. *Journal of Sound and Vibration*, 1989, 135: 1-19.

[5] Païdoussis,M.P., Li,G.X. and Rand,R.H., Chaotic motions of a constrained pipe conveying fluid: comparison between simulation, analysis and experiment. *Journal of Applied Mechanics*, 1991, 58: 559-565.

[6] Païdoussis,M.P., Cusumand,T.P. and Copeland,G.S., Low-dimensional chaos in a flexible tube conveying fluid. *Journal of Applied Mechanics*, 1992, 59: 196-205.

[7] Ni,Q. and Huang,Y.Y., Nonlinar dynamic analysis of a viscoelastic pipe conveying fluid. *China Ocean Engineering*, 2000, 14(3): 321-328.

[8] Jin,J.D., Stability and chaotic motions of a restrained pipe conveying fluid. *Journal of Sound and Vibration*, 1997, 208: 427-439.

[9] Wang,L. and Ni,Q., The nonlinear dynamic vibrations of a restrained pipe conveying fluid by differential quadrature method. *Journal of Dynamics and Control*, 2004, 2(4): 56-61 (in Chinese).

[10] Wang,L. and Ni,Q., A note on the stability and chaotic motions of a restrained pipe conveying fluid. *Journal of Sound and Vibration*, 2006, 296: 1079-1083

[11] Ni,Q., Wang,L. and Qian,Q., Chaotic transients in a curved fluid conveying tube. *Acta Mechanica Solida Sinica*, 2005, 18(3): 207-214.

[12] Ni,Q., Wang,L. and Qian,Q., Bifurcations and chaotic motions of a curved pipe conveying fluid with non-linear constraints. *Computers & Structures*, 2006, 84: 708-717.

[13] Païdoussis,M.P. and Issid,N.T., Dynamic stability of pipes conveying fluid. *Journal of Sound and Vibration*, 1976, 33: 267-294.

[14] Ni,Q. and Huang,Y.Y., Differential quadrature method to stability analysis of pipes conveying fluid with spring support. *Acta Mechanica Solida Sinica*, 2000, 13: 320-327.